

Morphology and Adhesion Strength of Myoblast Cells on Photocurable Gelatin under Native and Non-native Micromechanical Environments

Hiroshi Y. Yoshikawa,^{†,‡} Takahito Kawano,[§] Takehisa Matsuda,^{||} Satoru Kidoaki,^{*,§} and Motomu Tanaka^{*,†,⊥}

[†]Physical Chemistry of Biosystems, Institute of Physical Chemistry, University of Heidelberg, Heidelberg 69120, Germany

[‡]Department of Chemistry, Saitama University, Saitama 338-8570, Japan

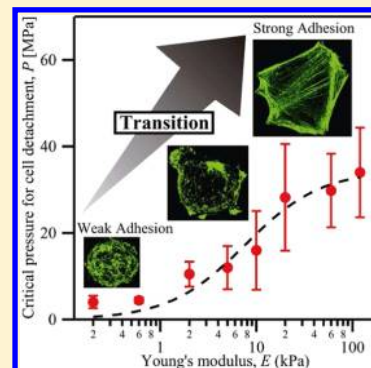
[§]Division of Biomolecular Chemistry, Institute for Materials Chemistry and Engineering, Kyushu University, Fukuoka 819-0395, Japan

^{||}Genome Biotechnology Laboratory, Kanazawa Institute of Technology, Ishikawa 924-0838, Japan

[⊥]Institute for Integrated Cell-Material Sciences (WPI iCeMS), Kyoto University, 606-8501, Kyoto, Japan

S Supporting Information

ABSTRACT: We have quantitatively determined how the morphology and adhesion strength of myoblast cells can be regulated by photocurable gelatin gels, whose mechanical properties can be fine-tuned by a factor of 10^3 ($0.1 \text{ kPa} \leq E \leq 140 \text{ kPa}$). The use of such gels allows for the investigation of mechanosensing of cells not only near the natural mechanical microenvironments ($E \sim 10 \text{ kPa}$) but also far below and beyond of the natural condition. Optical microscopy and statistical image analysis revealed that myoblast cells sensitively adopt their morphology in response to the substrate elasticity at $E \sim 1\text{--}20 \text{ kPa}$, which can be characterized by the significant changes in the contact area and order parameters of actin cytoskeletons. In contrast, the cells in contact with the gels with lower elastic moduli remained almost round, and the increase in the elasticity beyond $E \sim 20 \text{ kPa}$ caused no distinct change in morphology. In addition to the morphological analysis, the adhesion strength was quantitatively evaluated by measuring the critical detachment pressure with an aid of intensive pressure waves induced by picosecond laser pulses. This noninvasive technique utilizing extremely short pressure waves (pulse time width $\sim 100 \text{ ns}$) enables one to determine the critical pressure for cell detachment with reliable statistics while minimizing the artifacts arising from the inelastic deformation of cells. The adhesion strength also exhibited a transition from weak adhesion to strong adhesion within the same elasticity range ($E \sim 1\text{--}20 \text{ kPa}$). A clear correlation between the cell morphology and adhesion strength suggests the coupling of the strain of the substrate and the mechanosensors near focal adhesion sites.



INTRODUCTION

Adhesion of cells to extracellular matrix and neighboring cells is the first key step in the development process and maintenance of tissues. In nature, biochemical interaction between cells and their microenvironments are fine-tuned by the formation of ligand–receptor complexes. In addition, recent studies revealed that mechanical properties of the microenvironments also influence cell adhesion as well as many other cellular processes such as motility¹ and differentiation.² For instance, it has been reported that various cell types exhibit a clear increase in spreading (i.e., the area of cell–substrate contact) and stress fiber formation in contact with rigid, elastic substrates.^{2,3} In order to understand such mechanosensitive cell adhesion, chemically cross-linked hydrogels have been developed as the model of soft microenvironments for cells (extracellular matrix). The most widely used hydrogel to study matrix elasticity effects is polyacrylamide (PAA), but the surface of gels needs to be further functionalized with extracellular matrix

proteins, such as collagen and fibronectin, for the stable cell adhesion.⁴ As an alternative approach, tunable hydrogels based on naturally derived polymers such as gelatin,⁵ hyaluronic acid,⁶ and alginate⁷ are also used to mimic natural microenvironments. Recently, Kidoaki and Matsuda et al. reported that gelatin functionalized with styrene side chains can form curable gels, whose elastic modulus can be fine-adjusted simply by photo-cross-linking conditions.^{8–10} Moreover, since gelatin originates from extracellular collagen matrix, no additional chemical functionalization step is necessary. In a recent account, they reported that photo-cross-linked gelatin with elastic patterns can even mechanically guide the cell motility (mechanotaxis).⁹ They also reported that synchronized beating in culture cardiomyocyte tissue on photocurable gelatin can

Received: January 24, 2013

Revised: March 25, 2013

Published: March 26, 2013

significantly be modulated with substrate elasticity.¹⁰ These results clearly suggest that gelatin substrate elasticity significantly influence cell–substrate interaction, which plays key roles in regulating cell and tissue functions. However, the quantitative insights into the “strength” of interactions between cells and photocurable gelatin still remained unknown.

In this work, we have systematically evaluated cell adhesion to photocurable gelatin gels with different elastic moduli. By optimizing curing conditions, we achieved a finely tunable elasticity by a factor of 10^3 ($0.1 \text{ kPa} \leq E \leq 140 \text{ kPa}$). As the test cell system, we chose myoblast (C2C12) cells to gain a comprehensive view to the adhesion on soft and stiff substrates. The adhesion of C2C12 cells were investigated in terms of shape and morphology by optical microscopies. In addition, cell adhesion strength was quantitatively measured by the self-developed cell detachment assay, where the critical pressure for the cell detachment can be determined by pressure waves induced by picosecond laser pulses.^{11,12} In contrast to other techniques, such as pulling a cell with a magnetic tweezer¹³ or scratching a cell using an AFM tip,¹⁴ our “shock wave assay” is a probe-free technique that enables one to gain reliable statistics from many cells. Moreover, the duration of a force pulse is so short ($\Delta t \sim 100 \text{ ns}$) that experimental artifacts caused by shape adaptation and cytoskeleton remodeling during the measurements can be excluded. This ensures the quantitative measurement of strength of cell adhesion as a function of substrate elasticity.

■ EXPERIMENTAL SECTION

Preparation of Supporting Glass Substrate. A vinyl-silanized glass substrate was prepared for chemically fixing photocurable gelatin. Glass ($24 \text{ mm} \times 24 \text{ mm}$, thickness $0.12\text{--}0.17 \text{ mm}$) substrates were cleaned using a modified RCA method.¹⁵ The glass substrate were immersed in a 5% (v/v) toluene solution vinyltrimethoxysilane (Tokyo Chemical Industry Co. Ltd., Tokyo, Japan) and shaken for 18 h at room temperature. After the sequential rinsing with toluene, acetone, ethanol, and deionized water, the glass substrates were dried at $70 \text{ }^\circ\text{C}$ for 1 h in air.

Preparation of Photocurable Gel. Photocurable styrenated gelatin was prepared as previously described.^{8,9,16} Styrenated gelatin (30 wt %, degree of derivatization: 95%) and sulfonyl camphorquinone (2.5 wt % of gelatin; Toronto Research Chemicals, Ontario, Canada) were dissolved in phosphate-buffered saline (PBS). The mixed sol solution was centrifuged to remove colloidal coagulations. The sol solution was put onto glass substrate precoated with poly(*n*-isopropylacrylamide) (PNIPAAm, Sigma-Aldrich, Munich, Germany) on a hot plate at $45 \text{ }^\circ\text{C}$. Then the vinyl-silanized glass substrate was put over the sol solution. The sandwich-like sample was illuminated with white light ($\sim 3 \text{ mW/cm}^2$ measured at 550 nm) from a 120 W metal halide lamp (X-cite, Lumen Dynamics) for 20–500 s. Finally, the hardened gel was detached from the PNIPAAm-coated glass substrate in a PBS at $4 \text{ }^\circ\text{C}$ and then kept in PBS overnight with mild stirring at $20 \text{ }^\circ\text{C}$ to release PNIPAAm from the gel surface and make it swell sufficiently.

Measurement of Gels Elasticity. Elasticity of the gelatin gels was determined by nanoindentation analysis. Force–indentation (f – i) measurements were performed with an atomic force microscope (AFM) (NanoWizard, JPK Instruments, Berlin, Germany) in PBS. To compare nano- and microscale elastic properties of gels, two types of cantilevers

were used; silicon–nitride cantilever (spring constant of $0.01\text{--}1.0 \text{ N/m}$, Veeco Instruments, Mannheim, Germany) with (1) a half-pyramidal tip or (2) a microparticle. Silica glass spheres (diameter: $5 \text{ }\mu\text{m}$) were glued on a cantilever with water insoluble epoxy (endfest 300, UHU, Germany). In the case of pyramidal tips, the Young’s modulus, E , of gelatin gels was determined by fitting f – i curves with Sneddon’s modification of the Hertz model:¹⁷

$$F = \frac{2 \tan(\alpha)}{\pi} \frac{E}{1 - \mu^2} \delta^2 \quad (1)$$

where F is the load, δ the indentation depth, μ the Poisson ratio, and α a semivertical angle of the indenter. On the other hand, f – i curves obtained with a particle-tipped cantilever were fitted with the Hertz model:¹⁸

$$F = \frac{4}{3} \frac{E}{1 - \mu^2} \sqrt{R} \delta^{3/2} \quad (2)$$

where R is the radius the indenting sphere. In this study, μ and α were assumed to be 0.5 and 35° , respectively.

Cell Culture. The mouse myoblast cell line (C2C12, <20 passage) purchased from DSMZ GmbH (Braunschweig, Germany) was maintained in polystyrene flasks in a $37 \text{ }^\circ\text{C}$ incubator and cultured in RPMI-1640 media modified with HEPES (Sigma-Aldrich, Germany) supplemented with 10% of fetal bovine serum (PAA laboratories, Cölbe, Germany) 20 U/mL penicillin and $100 \text{ }\mu\text{g}/\mu\text{L}$ streptomycin (PAA Laboratories). The gelatin gel substrate was immersed overnight with RPMI-1640 media, and then cells were seeded onto the gelatin gel substrate in a plastic Petri dish and cultured in a $37 \text{ }^\circ\text{C}$ incubator. After 30 min, the gelatin gel substrate was placed in custom-made Petri dishes with glass coverslip bottom (diameter 40 mm , thickness $0.12\text{--}0.17 \text{ mm}$) and cultured with a fresh RPMI-1640 medium.

Image Acquisition and Analysis of Cells. The adhesion behavior of cells on the gelatin gel was monitored using an inverted microscope (TE-2000U, Nikon Instruments Inc.) with a custom-made temperature-controllable cell chamber. Cell images were recorded with a CCD camera (A602f, Basler, Ahrensburg, Germany). The projected area, elongation (length/width ratio defined by ellipsoidal fitting), and circularity ($4\pi \times (\text{projected area})/(\text{perimeter})^2$) of the adherent cells were calculated using image analysis software, ImageJ. For confocal fluorescence microscopy, cells cultured for either 2 or 24 h culture were fixed with 4% formaldehyde for 20 min at room temperature. Then the cells were permeabilized using 0.1% Triton X-100 surfactant in phosphate buffer saline (PBS) for 3 min. Finally, cells were incubated in Alexa 488-conjugated phalloidin (Invitrogen) and 1% bovine serum albumin in PBS for 20 min. The samples were mounted onto coverslips in PBS and viewed with a laser-scanning confocal microscope (A1R, Nikon Instruments Inc.) with a $60\times$ objective (N.A. = 1.2, water immersion, Nikon Instruments Inc.). The resulting confocal images were deconvoluted using Huygens deconvolution software (Scientific Volume Imaging, Netherlands). The maximum projection images along the optical axis (z -axis) were used for the calculation of order parameter of actin fibers. The algorithm uses a series of elongated Laplace of Gaussian filters to create a maximum response image as described by Zemel et al.¹⁹ First, n anisotropic Gaussian of the following forms

$$G = \frac{1}{2\pi\sigma_x\sigma_y} e^{-(x^2/2\sigma_x^2 + y^2/2\sigma_y^2)} \quad (3)$$

were generated and each rotated in steps of π/n from 0 to $\pi - \pi/n$. In this work, $n = 15$ and multiple values for σ_x and σ_y were used. The Gaussian kernels are then convoluted with the Laplacian filter given by

$$\mathbf{L} = \begin{pmatrix} 0 & -1 & 0 \\ -1 & 4 & -1 \\ 0 & -1 & 0 \end{pmatrix} \quad (4)$$

The n eLoG kernels are each convoluted with the original fluorescence images to produce n response images. The maximum over the n response images at each xy pixel was used to create a maximum response image. This maximum image is then processed by an intensity threshold to yield the binary mask of the segmented stress fibers. In addition, round bodies smaller than 50 pixels were removed from the image to cut off nonfibrous actin clusters. Finally, the order parameter was determined from the histogram of pixel numbers multiplied by the corresponding fluorescence intensities (and thus the amount of actin fibers) for each orientation.

Topography of the fixed cells on gels was also acquired with the atomic force microscope. Silicon nitride cantilever (0.01 N/m, Veeco Instruments, Mannheim, Germany) was scanned with a contact mode with a force below 200 pN.

Picosecond Laser Cell Detachment Assay. The experimental system for the measurement of cell adhesion strength by picosecond laser-induced shock wave was described in our previous report.^{11,12} A picosecond Nd:YAG laser system ($\lambda = 1064$ nm, $\tau = 60$ ps, PY 61C-20, Continuum, Santa Clara, CA) was used to induce shock waves. The picosecond laser pulses were led through an inverted microscope and focused through a 20 \times objective lens (N.A. = 0.75, Nikon Instruments Inc.). A single picosecond laser pulse was focused into a culture medium at a distance of 1.3, 1.5, or 2 mm from cells and 100 μm above a gelatin surface. The laser energy was adjusted with a polarizer and measured with a power meter (PE 10-S, OPHIR). The minimum energy needed to detach cells from substrate is defined as the critical detachment energy. This parameter was determined by systematically varying the detachment energy until the minimum threshold value was achieved for cell detachment from the substrate. The corresponding critical pressure (i.e., the minimum pressure required for cell detachment) was then calculated from the energy–pressure curve obtained in water using a factory-calibrated pressure sensor (Müller-Platte Needleprobe, Müller Instruments, Oberursel, Germany).

RESULTS AND DISCUSSION

Elastic Properties of Photocurable Gelatin Gels. Figure 1a shows the force–indentation ($f-i$) curves of photocurable gelatin gels (irradiation time = 35 s) measured by a cantilever with a pyramidal tip or a microparticle. Since typical thickness of the hydrated gelatin gels in this study is over 50 μm , the fitting analysis up to $\delta = 1$ μm (i.e., less than 2% of the gel thickness) of the $f-i$ curves can determine E values that were independent of the underlying stiff glass substrate.^{20,21} In fact, the $f-i$ curves were fit well by the Hertz cone and sphere models. The both fittings yielded same elastic modulus, $E = 6.3$ kPa, indicating uniformity of elastic properties of the gelatin gels in the dimension from nanometers to micrometers. Figure

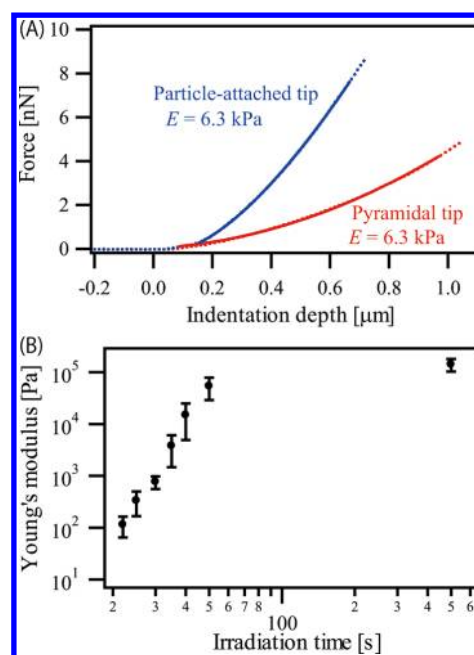


Figure 1. Evaluation of photocurable gelatin gel by AFM. (A) Force–indentation ($f-i$) curves of gelatin gels (irradiation time = 35 s) measured by a cantilever with a pyramidal tip or a microparticle (diameter: 5 μm). (B) Elasticity of the gelatin gels as a function of irradiation time.

1b shows elasticity of the gelatin gels as a function of light irradiation time. The gelatin gels exhibited a drastic change in the Young's modulus by a factor of 10^3 (0.1 kPa $\leq E \leq 140$ kPa) depending on the irradiation time from 20 to 500 s. This is a relatively large range compared to most other polymer systems²² and comparable with polyacrylamide (PAA) systems,² which is based on synthetic molecules. In addition, this covers the optimal elasticity for striation of C2C12 myotubes ($E = 12-15$ kPa)⁴ and enables us to investigate adhesion behavior of C2C12 cells with significantly softer and stiffer conditions as well as the optimal elastic conditions.

Evaluation of Cell Shapes and Morphology. Figure 2 shows representative phase contrast images of C2C12 cells cultured on (A) soft ($E = 0.8$ kPa) and (B) stiff ($E = 140$ kPa) gels for 3 and 24 h. C2C12 cells exhibit a pronounced spreading on a stiff gel after 3 h, as reported for many

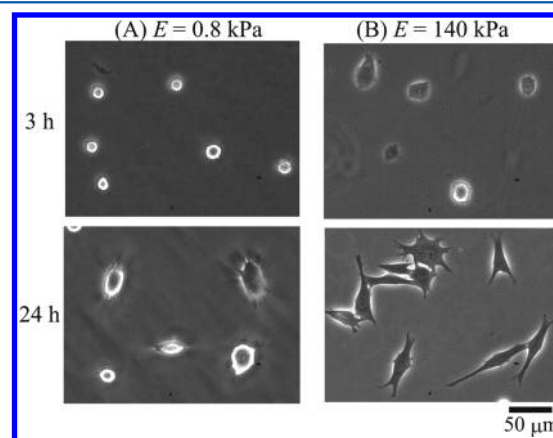


Figure 2. Phase contrast images of C2C12 cells ($t = 3$ and 24 h) cultured on gelatin gels at $E =$ (A) 0.8 kPa and (B) 140 kPa.

contractile cells on stiff substrates.^{16,17,23} After 24 h, the shape of C2C12 cells on the soft gels was still nearly round, whereas the cells on the stiff gels were significantly elongated. The statistical analysis of the cell shape with two structural measures, elongation and circularity, also showed distinct differences (Table 1). Figure 3 represents the topographical

Table 1. Elongation (Length/Width Ratio Defined by Ellipsoidal Fitting) and Circularity ($4\pi \times (\text{Projected Area})/(\text{Perimeter})^2$) of C2C12 Cells on Gelatin Gels at (A) $E = 0.8$ kPa and (B) 140 kPa after 3 and 24 h of Incubation

	$E = 0.8$ kPa		$E = 140$ kPa	
	3 h	24 h	3 h	24 h
elongation	1.19 ± 0.19	2.00 ± 0.97	1.59 ± 0.53	3.02 ± 1.69
circularity	0.72 ± 0.18	0.52 ± 0.20	0.70 ± 0.17	0.29 ± 0.14

images of cells on soft and stiff gels. On soft gelatin gels with $E = 0.8$ kPa (Figure 3A), wrinkles were formed around the edge of cells, which is caused by contraction forces generated by the cell.⁵ It should be noted that the relative depth of wrinkles with respect to the flat gel surfaces was $\sim 5 \mu\text{m}$, which is significantly larger than that reported for fibroblasts adhering to a 5 kPa PA gel ($\leq 1 \mu\text{m}$).²⁴ On the other hand, on stiff gels with $E = 140$ kPa, we observed no sign of topographic change caused by the adherent cells (Figure 3B).

Figure 4 shows the characteristic morphology of C2C12 cells on the gelatin gels with a wider range of elastic moduli, $E \sim 0.1$ –140 kPa. The cells were fixed 2 and 24 h after the seeding, and the actin cytoskeletons were labeled with phalloidin conjugated with Alexa 488 dye. At $t = 2$ h, cells on the softest gel ($E \sim 0.1$ kPa) showed almost a round shape, having a little contact area to the substrate. The same tendency was observed for gels with $E \sim 1$ and 5 kPa; cells are hemispheres with spreading fronts. According to the further increase in the substrate elasticity, we observed a clear tendency that the spreading becomes more pronounced. At the initial phase of cell–substrate contact ($t = 2$ h), the spreading of cells seems to be isotropic, which shares a common feature with the morphology of cancer cells observed during the early stage of cell–substrate contacts.²⁵ On the substrate with $E \geq 10$ kPa, the cells take polygonal shapes, showing a clear accumulation of actin meshwork near the cell periphery with a few stress fibers. After 24 h, the cells on soft gelatin gels ($E \sim 0.1$ kPa) remain isotropic, but the global shape of cells on the gels with $E \geq 5$ kPa becomes clearly anisotropic. In contrast to the corresponding images at $t = 2$ h, the cells take much more spiky shape,

stretching many filopodia. To quantitatively determine the influence of substrate elasticity on remodeling of actin cytoskeletons, the order parameter of actin fibers ($S = \langle \cos 2\theta \rangle$) was calculated. Here, θ is the angle between each actin fibers in the cell and the long axis of the fitted ellipse. The amount of actin fibers at each orientation was identified by the image analysis with a series of eLoG filters (Figure S1). As presented in Figure 4, we observed a clear impact of the substrate elasticity on the cytoskeletal ordering. A clear increase in the order parameter S (> 0.1) was observed according to an increase in the substrate stiffness and a prolonged incubation time.

The change in cell morphology on photo-cross-linked gelatin surfaces was statistically analyzed by plotting the projected area of cells at $t = 3$ h as a function of elastic modulus (Figure 5). As presented in the figure, the projected area of cells increased approximately from 300 to 900 μm^2 according to the increase in the stiffness from 0.6 to 140 kPa. The obtained results are well fitted with the empirical Hill equation:^{3,4}

$$\text{Area} = aE^m / [(E_{1/2\text{-spread}})^m + E^m] \quad (5)$$

where $E_{1/2\text{-spread}}$ is the half-saturation constant for cell spreading and m is the cooperativity coefficient. Here we fitted the plot in the E range only from 0.8 to 140 kPa. In fact, since cells on the gels with low elastic modulus ($E \leq 1$ kPa) have contact angles over 90° (Figure 4), the project area does not correspond to the contact area between cells and gels. The fitting of the experimental results (solid line, Figure 5) yields $E_{1/2\text{-spread}} = 1.8$ kPa, and $m = 1.1$. $E_{1/2\text{-spread}}$ can be used as a criterion for cell spreading: substrates with $E \geq E_{1/2\text{-spread}}$ facilitate cell spreading, while softer substrates ($E < E_{1/2\text{-spread}}$) elicit little cell spreading. The cooperativity coefficient, $m \sim 1$, indicates minimal cooperativity. These values seem to be in agreement with the previous report on C2C12 cells on polyacrylamide gels functionalized with type I collagen, $E_{1/2\text{-spread}} = 2.4$ –5.1 kPa and $m \sim 1$.⁴ Since gelatin is a hydrolyzed form of collagen lacking the specific binding capability to integrin,^{23,26,27} the clear adhesion observed in this study can be attributed to the adsorbed serum proteins, such as fibronectin that specifically binds to integrin.²⁸ In fact, Kidoaki et al. previously reported that the surface density of serum proteins adsorbed on gelatin surfaces does not depend on the gel elasticity.⁹ Thus, we can conclude that the difference in cell morphology is dominated by the mechanical properties of gelatin gels.

Evaluation of Cell Adhesion Strength. The results of optical microscopy clearly showed a significant impact of gelatin substrate elasticity on cell morphology. Such substrate

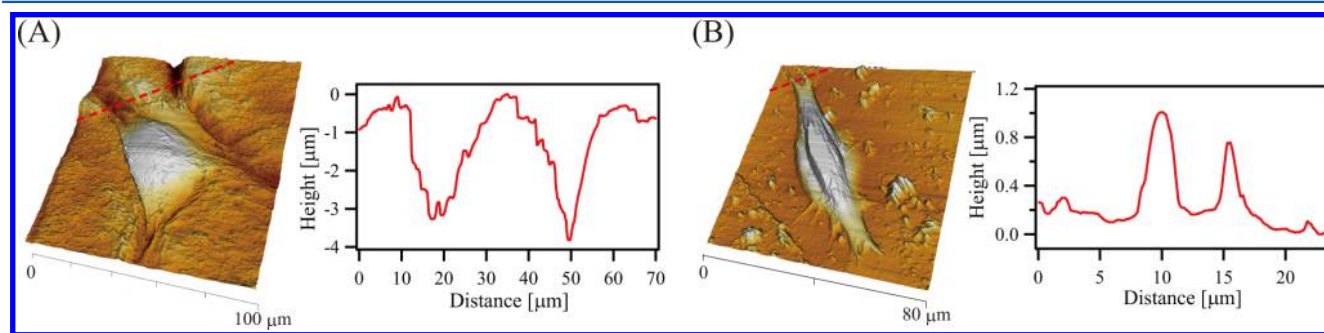


Figure 3. Topographical map of C2C12 cells cultured for 24 h on gelatin gels at $E =$ (A) 0.8 kPa and (B) 140 kPa. The plots represent the depth profile along the solid line (red) in the topographical images. The cells were fixed with 4% formaldehyde and imaged with AFM in PBS.

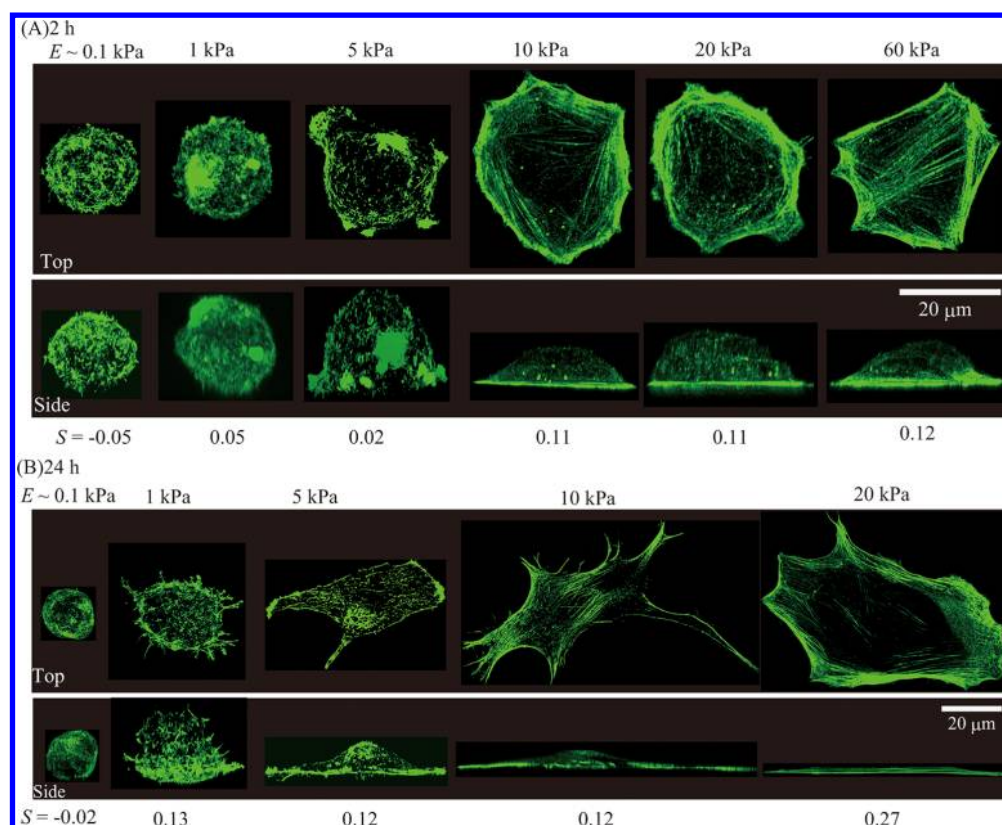


Figure 4. Confocal fluorescence images obtained for C2C12 cells on gelatin gels after 2 h (upper rows) at $E \sim 0.1$ –60 kPa and 24 h (lower rows) at $E \sim 0.1$ –20 kPa. Prior to imaging, the cells were fixed 4% formaldehyde and stained with Alexa 488 phalloidin. The images represent maximal projection along the optical axis (z -axis, top) and a side projection (y -axis, side). Actin fiber order parameters ($S = \langle \cos 2\theta \rangle$) calculated from each image are given below the images.

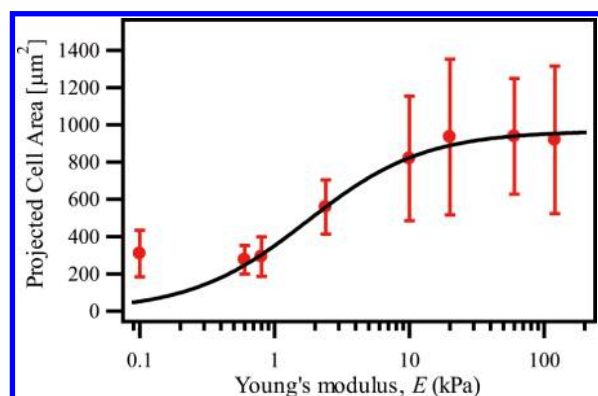


Figure 5. Projected area of C2C12 cells as a function of gel elasticity ($t \sim 3$ h). Error bars represent the standard deviations. The plot was fit with the Hill equation (eq 5) in the E range from 0.8 to 140 kPa, and the fitting curve was extrapolated to the E larger range.

elasticity-dependent cell morphology is consistent with those with other hydrogels, indicating that cell–substrate interactions are significantly influenced simply by the substrate elasticity. However, quantitative insights into cell–substrate adhesion strength as a function of substrate elasticity have not been investigated in a quantitative manner. To evaluate the strength of cell adhesion on photocurable gelatin gels, we utilized pressure waves induced by picosecond laser pulses.¹¹ Here, the critical pressure required to cause the detachment of adherent cells P_{th} can be used as a “mechanical” measure to quantitatively assess how strongly the cell–substrate interaction (adhesion) is

influenced by substrate mechanics. Figure 6 represents the bright-field microscopy images of C2C12 cells on gelatin gels before and after the detachment. Here, the critical detachment pressures of $P_{th} = 3.4$ or 8.1 MPa can be determined for gels with $E = 0.6$ and 10 kPa, respectively (Figure 6). The value

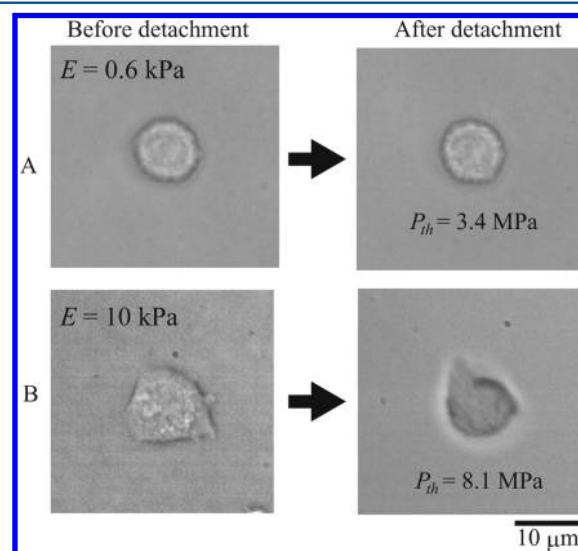


Figure 6. Bright-field images of an individual cell on gelatin gel at $E =$ (A) 0.6 kPa and (B) 10 kPa before (left) and after (right) its detachment when subjected to a shock wave above a certain minimum pressure.

obtained here is ~ 2 times bigger than the corresponding values on PDPA₅₀-PMPC₂₅₀-PDPA₅₀ films,¹¹ which can be attributed to the enhanced adhesion via adsorption of serum fibronectin to gelatin.

Figure 7A shows the average pressure as a function of gel elasticity, E , at $t = 3$ h. The average of P_{th} increased from 4.1 to

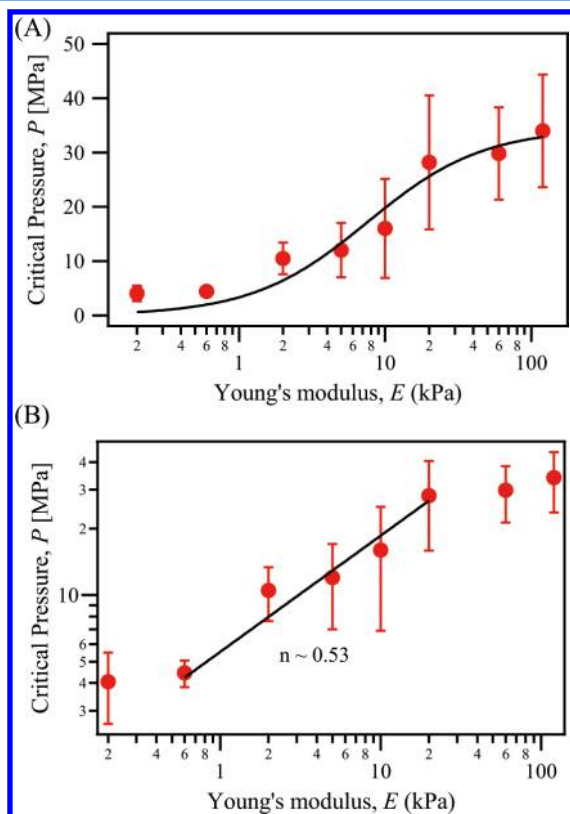


Figure 7. Evaluation of adhesion strength of C2C12 cells on gelatin gels. (A) The average of critical pressure as a function of gel elasticity at $t \sim 3$ h. The black solid line is the fitting with the Hill equation (eq 6). The error bar represents standard deviation. (B) Log–log plots converted from the plot of (A). The black solid line represents the fitting with the power law function (eq 7).

34 MPa according to the increase in the stiffness, 0.2 to 140 kPa. The monotonic increase in the adhesion strength of C2C12 cells is in good agreement with the past studies by micropipets,^{4,29} but we found that the transition from weak adhesion ($P_{\text{th}} < 5$ MPa) to strong adhesion ($P_{\text{th}} > 20$ MPa) takes place in a narrower E range ($1 \text{ kPa} \leq E \leq 20 \text{ kPa}$). Since the global shape of transition share some common features with changes in the projected area of cells (Figure 5), we fitted the results with the empirical Hill equation.

$$P_{\text{th}} = bE^m / [(E_{1/2-\text{adhesion}})^m + E^m] \quad (6)$$

As indicated by the solid line, the fit with the cooperativity coefficient taken from the projected area ($m = 1.1$) can well represent the experimental results. The half-saturation level $E_{1/2-\text{adhesion}} \sim 7.6$ kPa is about 3 times larger than that in the projected area analysis, but it should be noted that these two values obtained from the empirical analyses are not physically corresponding with each other.

To date, several studies reported that cell morphological processes that include cytoskeletons can phenomenologically be analyzed with power laws, such as the dependence of

viscosity of cytoplasm on shear rate,³⁰ the dependence of projected area of smooth muscle cells on the substrate elasticity,³ and the dependence of transit time of leukocytes through narrow pores.³¹ Figure 7B represents the log–log plot of P_{th} vs E for the regime in which the transition was observed: $0.6 \text{ kPa} \leq E \leq 20 \text{ kPa}$. The solid line corresponds to the power law:

$$P_{\text{th}} = cE^n \quad (7)$$

The obtained power law exponent, $n \sim 0.53$, may be attributed to the establishment of firm adhesion by the formation of stress fibers bound to focal adhesions via talin.^{32,33} Here, contraction force generated by focal adhesions activate the Src kinase, leading to an increase in the adhesion strength.³⁴ In fact, the range of elastic modulus ($0.6 \text{ kPa} \leq E \leq 20 \text{ kPa}$) agreed very well with the regime where the stress fiber formation was observed by confocal microscopy (Figure 4). Such a power law model can also be applied for the analysis of the projected area of cells at $0.8 \text{ kPa} \leq E \leq 20 \text{ kPa}$, yielding an exponent of $n \sim 0.31$ (Figure S2). The observed power law dependences suggest the transition from weak to strong adhesion can be correlated with the stress fiber formation. Thus, it is plausible that the traction force exerted by cells at $E \sim 1$ kPa reaches the critical threshold for the activation of mechanoreceptors. On the other hand, the small change in the projected area of adhesion and critical detachment pressures on gels with $E \geq 20$ kPa suggests that the activation of mechanosensors of C2C12 cells is already saturated at $E \sim 20$ kPa.

CONCLUSIONS

We systematically investigated the impact of mechanical properties of photocurable gelatin gels on the morphology and adhesion strength of myoblast cells. Nano- and micro-indentation experiments with AFM revealed that the optimization of the photo-cross-linking reactions enables one to fine-adjust the mechanical properties of gelatin gels by a factor of 10^3 ($0.1 \text{ kPa} \leq E \leq 140 \text{ kPa}$). Confocal microscopy images of cells labeled with dye-conjugated phalloidin revealed that myoblast cells can adopt their morphology to the elastic modulus of substrates, showing clear differences in the remodeling of actin cytoskeletons. On gels with low elasticity ($E < 1$ kPa), cells remained (hemi)spherical and exhibited a uniform distribution of actins in the cytoplasmic space. An increase in the substrate elasticity leads to a more pronounced and isotropic cell spreading. On the substrate with $E \geq 10$ kPa, the cells take polygonal shapes at $t = 2$ h, showing a clear accumulation of actin meshwork near the cell periphery. After 24 h, the cells on gels with $E < 1$ kPa remain isotropic, while the cells on the gels with $E > 5$ kPa take much more spiky shape, stretching many filopodia. The projected contact area between cells and substrates can be well analyzed by the empirical Hill equation, demonstrating that the adhesion is a cooperative process. With an aid of intensive pressure waves generated by picosecond laser pulses, the critical pressure to detach the adherent cells from gelatin gels could quantitatively be determined as a function of substrate elasticity. After 3 h, we observed a distinct transition from weak to strong adhesion in the range of elastic modulus ($1 \text{ kPa} \leq E \leq 20 \text{ kPa}$), where we found a power law relationship between the critical detachment pressure and the elasticity. In nature, myoblast cells live in the mechanical environments with $E \sim 10$ kPa. Engler et al. also reported that an optimal elastic modulus of $E \sim 12$ kPa maximizes myosin striations in muscle.⁴ Interestingly, the

adhesion strength obtained at comparable elasticity ($E \sim 10$ kPa) is almost at the middle of the adhesion strength transition, which is a quantitative insight into optimal cell–substrate interaction for cell functions. In addition, such a high mechanosensitivity in the range of elastic modulus ($1 \text{ kPa} \leq E \leq 20 \text{ kPa}$) can be correlated with the formation of stress fibers caused by the mechanoreceptors at focal adhesion sites. Thus, in future, simultaneous measurements of adhesion strength and focal adhesion size would be interesting to understand mechanosensitive cell–substrate interactions. We believe that our approach with the combination of photocurable gelatin, image analysis, and the pressure wave assays is powerful to correlate morphology and cell adhesion strength on fine-tunable micromechanical environments.

■ ASSOCIATED CONTENT

Supporting Information

Representative results of image analysis for the actin fiber orientation and a log–log plot of projected area of C2C12 cells as a function of gel elasticity. This material is available free of charge via the Internet at <http://pubs.acs.org>.

■ AUTHOR INFORMATION

Corresponding Author

*Tel +81-(0)-92-802-2507, Fax +81-(0)-92-802-2509, e-mail kidoaki@ms.ifoc.kyushu-u.ac.jp (S.K.); Tel +49-(0)-6221-544916, Fax +49-(0)-6221-544918, e-mail tanaka@uni-heidelberg.de (M.T.).

Notes

The authors declare no competing financial interest.

■ ACKNOWLEDGMENTS

M.T. thanks the German Science Foundation (SFB 873) for the support and K. Yoshikawa for stimulating discussions. H.Y.Y. thanks the Alexander von Humboldt Foundation for a research fellowship and Japan Society for the Promotion of Science for the support by KAKENHI (No. 24680050, 24106505, and 24656006). M.T. is a member of the German Excellence Cluster “CellNetwork” and the Helmholtz Program “BioInterface”. We thank A. Antunes and A. Baser for the support on preparations of gels and particle-attached cantilevers and W. Abuillan for the insightful discussion about image analysis.

■ REFERENCES

- (1) Pelham, R. J.; Wang, Y. L. Cell Locomotion and Focal Adhesions Are Regulated by Substrate Flexibility. *Proc. Natl. Acad. Sci. U. S. A.* **1997**, *94*, 13661–13665.
- (2) Engler, A. J.; Sen, S.; Sweeney, H. L.; Discher, D. E. Matrix Elasticity Directs Stem Cell Lineage Specification. *Cell* **2006**, *126*, 677–689.
- (3) Engler, A.; Bacakova, L.; Newman, C.; Hategan, A.; Griffin, M.; Discher, D. Substrate Compliance versus Ligand Density in Cell on Gel Responses. *Biophys. J.* **2004**, *86*, 388a–388a.
- (4) Engler, A. J.; Griffin, M. A.; Sen, S.; Bonnetnann, C. G.; Sweeney, H. L.; Discher, D. E. Myotubes Differentiate Optimally on Substrates with Tissue-Like Stiffness: Pathological Implications for Soft or Stiff Microenvironments. *J. Cell Biol.* **2004**, *166*, 877–887.
- (5) Harris, A. K.; Wild, P.; Stopak, D. Silicone-Rubber Substrata - New Wrinkle in the Study of Cell Locomotion. *Science* **1980**, *208*, 177–179.
- (6) Rehfeldt, F.; Brown, A. E.; Raab, M.; Cai, S.; Zajac, A. L.; Zemel, A.; Discher, D. E. Hyaluronic Acid Matrices Show Matrix Stiffness in

2d and 3d Dictates Cytoskeletal Order and Myosin-II Phosphorylation within Stem Cells. *Integr. Biol.* **2012**, *4*, 422–430.

(7) Augst, A. D.; Kong, H. J.; Mooney, D. J. Alginate Hydrogels as Biomaterials. *Macromol. Biosci.* **2006**, *6*, 623–633.

(8) Kidoaki, A.; Matsuda, T. Microelastic Gradient Gelatinous Gels To Induce Cellular Mechanotaxis. *J. Biotechnol.* **2008**, *133*, 225–230.

(9) Kawano, T.; Kidoaki, S. Elasticity Boundary Conditions Required for Cell Mechanotaxis on Microelastically-Patterned Gels. *Biomaterials* **2011**, *32*, 2725–2733.

(10) Horning, M.; Kidoaki, S.; Kawano, T.; Yoshikawa, K. Rigidity Matching Between Cells and the Extracellular Matrix Leads to the Stabilization of Cardiac Conduction. *Biophys. J.* **2012**, *102*, 379–387.

(11) Yoshikawa, H. Y.; Rossetti, F. F.; Kaufmann, S.; Kaindl, T.; Madsen, J.; Engel, U.; Lewis, A. L.; Armes, S. P.; Tanaka, M. Quantitative Evaluation of Mechanosensing of Cells on Dynamically Tunable Hydrogels. *J. Am. Chem. Soc.* **2011**, *133*, 1367–1374.

(12) Yoshikawa, H. Y.; Cui, J.; Kratz, K.; Matsuzaki, T.; Nakabayashi, S.; Marx, A.; Engel, U.; Lendlein, A.; Tanaka, M. Quantitative Evaluation of Adhesion of Osteosarcoma Cells to Hydrophobic Polymer Substrate with Tunable Elasticity. *J. Phys. Chem. B* **2012**, *116*, 8024–8030.

(13) Bausch, A. R.; Moller, W.; Sackmann, E. Measurement of Local Viscoelasticity and Forces in Living Cells by Magnetic Tweezers. *Biophys. J.* **1999**, *76*, 573–579.

(14) Yamamoto, A.; Mishima, S.; Maruyama, N.; Sumita, M. A New Technique for Direct Measurement of the Shear Force Necessary To Detach a Cell from a Material. *Biomaterials* **1998**, *19*, 871–879.

(15) Kern, W.; Puotinen, D. A. Cleaning Solutions Based on Hydrogen Peroxide for Use in Silicon Semiconductor Technology. *RCA Rev.* **1970**, *31*, 187–207.

(16) Okino, H.; Nakayama, Y.; Tanaka, M.; Matsuda, T. In Situ Hydrogelation of Photocurable Gelatin and Drug Release. *J. Biomed. Mater. Res.* **2002**, *59*, 233–245.

(17) Sneddon, I. N. The Relation Between Load and Penetration in the Axisymmetric Boussinesq Problem for a Punch of Arbitrary Profile. *Int. J. Eng. Sci.* **1965**, *3*, 47–57.

(18) Hertz, H. Über Die Berührung Fester Elastischer Körper. *Zh. Reine Angew. Math.* **1882**, *92*, 156–171.

(19) Zemel, A.; Rehfeldt, F.; Brown, A. E. X.; Discher, D. E.; Safran, S. A. Optimal Matrix Rigidity for Stress-Fibre Polarization in Stem Cells. *Nat. Phys.* **2010**, *6*, 468–473.

(20) Domke, J.; Radmacher, M. Measuring the Elastic Properties of Thin Polymer Films with the Atomic Force Microscope. *Langmuir* **1998**, *14*, 3320–3325.

(21) Rotsch, C.; Jacobson, K.; Radmacher, M. Dimensional and Mechanical Dynamics of Active and Stable Edges in Motile Fibroblasts Investigated by Using Atomic Force Microscopy. *Proc. Natl. Acad. Sci. U. S. A.* **1999**, *96*, 921–926.

(22) Rehfeldt, F.; Engler, A. J.; Eckhardt, A.; Ahmed, F.; Discher, D. E. Cell Responses to the Mechanochemical Microenvironment—Implications for Regenerative Medicine and Drug Delivery. *Adv. Drug Delivery. Rev.* **2007**, *59*, 1329–1339.

(23) Tuckwell, D. S.; Ayad, S.; Grant, M. E.; Takigawa, M.; Humphries, M. J. Conformation Dependence of Integrin-Type-II Collagen-Binding - Inability of Collagen Peptides To Support Alpha(2)Beta(1) Binding, and Mediation of Adhesion to Denatured Collagen by a Novel Alpha(5)Beta(1)-Fibronectin Bridge. *J. Cell Sci.* **1994**, *107*, 993–1005.

(24) Solon, J.; Levental, I.; Sengupta, K.; Georges, P. C.; Janmey, P. A. Fibroblast Adaptation and Stiffness Matching to Soft Elastic Substrates. *Biophys. J.* **2007**, *93*, 4453–4461.

(25) Kaindl, T.; Rieger, H.; Kaschel, L. M.; Engel, U.; Schmaus, A.; Sleeman, J.; Tanaka, M. Spatio-Temporal Patterns of Pancreatic Cancer Cells Expressing Cd44 Isoforms on Supported Membranes Displaying Hyaluronic Acid Oligomers Arrays. *PLoS One* **2012**, *7*.

(26) Davis, G. E. Affinity of Integrins for Damaged Extracellular-Matrix - Alpha-V-Beta-3 Binds to Denatured Collagen Type-I through Rgd Sites. *Biochem. Biophys. Res. Commun.* **1992**, *182*, 1025–1031.

- (27) Jones, P. L.; Crack, J.; Rabinovitch, M. Regulation of Tenascin-C, a Vascular Smooth Muscle Cell Survival Factor That Interacts with the Alpha(V)Beta(3) Integrin To Promote Epidermal Growth Factor Receptor Phosphorylation and Growth. *J. Cell Biol.* **1997**, *139*, 279–293.
- (28) Pankov, R.; Yamada, K. M. Fibronectin at a Glance. *J. Cell Sci.* **2002**, *115*, 3861–3863.
- (29) Griffin, M. A.; Engler, A. J.; Barber, T. A.; Healy, K. E.; Sweeney, H. L.; Discher, D. E. Patterning, Prestress, and Peeling Dynamics of Myocytes. *Biophys. J.* **2004**, *86*, 1209–1222.
- (30) Tsai, M. A.; Waugh, R. E.; Keng, P. C. Cell Cycle-Dependence of HI-60 Cell Deformability. *Biophys. J.* **1996**, *70*, 2023–2029.
- (31) Nossal, R. Cell Transit Analysis of Ligand-Induced Stiffening of Polymorphonuclear Leukocytes. *Biophys. J.* **1998**, *75*, 1541–1552.
- (32) Burridge, K.; Connell, L. A New Protein of Adhesion Plaques and Ruffling Membranes. *J. Cell Biol.* **1983**, *97*, 359–367.
- (33) Kaufmann, S.; Piekenbrock, T.; Goldmann, W. H.; Barmann, M.; Isenberg, G. Talin Binds to Actin and Promotes Filament Nucleation. *FEBS Lett.* **1991**, *284*, 187–191.
- (34) Vogel, V.; Sheetz, M. Local Force and Geometry Sensing Regulate Cell Functions. *Nat. Rev. Mol. Cell Biol.* **2006**, *7*, 265–275.